

Cosmological Simulations of Multi-Component Cold Dark Matter

Mikhail V. Medvedev*

Institute for Theory and Computation, Harvard University, 60 Garden St., Cambridge, MA 02138[†]

The nature of dark matter is unknown. A number of dark matter candidates are quantum flavor-mixed particles but this property has never been accounted for in cosmology. Here we explore this possibility from the first principles via extensive N -body cosmological simulations and demonstrate that the two-component dark matter model agrees with observational data at all scales. Substantial reduction of substructure and flattening of density profiles in the centers of dark matter halos found in simulations simultaneously resolve several outstanding puzzles of modern cosmology. Predictions for direct and indirect detection dark matter experiments are also made.

PACS numbers: 95.35.+d, 95.30.Cq, 98.80.-k, 14.80.-j

Dark matter (DM) constitutes about 80% of matter and 25% of the total energy density in the universe but its nature remains completely unknown. The existence of DM requires revision of the present day physics. Most likely, DM is a hypothetical particle or particles beyond the standard model [1].

The current heuristic paradigm of cold dark matter with a cosmological constant (Λ CDM) is very successful at reproducing the large-scale structure of the universe but appears to disagree with observations on small scales. First, simulations predict the overabundance of small mass (dwarf) halos as compared to the much lower number of the observed satellite galaxies in the Local Group [2–5] and in the field as inferred from ALFALFA survey [6]. This problem was termed the “substructure problem” or the “missing satellite problem.” Second, the cuspy $\rho \propto r^{-1}$ DM density profiles in Λ CDM simulations [7] disagree with rotation curves of dwarf and low surface brightness galaxies, which indicate flattened or cored density profiles [8–10]. Observations of galaxy clusters also indicate the presence of cores [11]. Moreover, the largest CDM subhalos in the Local Group-type environments are too dense in their centers to host any of the dwarf spheroidal galaxies around the Milky Way or Andromeda galaxies [12, 13]. These two, perhaps related, “inner halo problems” are known as the “core-cusp problem” and the “too big to fail problem”, respectively. Importantly, numerous attempts to reconcile the Λ CDM model with observations using baryonic processes made so far (modified star formation, tidal gas stripping, supernova feedback) are unconvincing [4, 14–18]. This is because the inner halo problems require strong feedback and, hence, larger star formation whereas the missing satellite problem requires the star formation to be suppressed. Contrary to early expectations, a mild modification of the DM paradigm to adopt the warm DM model [19, 20] also fails to resolve all these problems altogether [21–23] due to similar constraints on the DM mass.

The inability of conventional physics to resolve aforementioned problems within the collisionless CDM paradigm indicates that cosmological DM exhibits non-gravitational properties as well. The most natural alter-

native is to admit a large interaction cross-section of DM with itself [24, 25] but not with normal matter. Contrary to early claims [26–28], such self-interacting dark matter (SIDM) was successful to explain the origin of cores provided certain constraints on the velocity-dependent cross-section $\sigma(v)$ are satisfied [29–35]; however it completely fails to solve the missing satellite problem [34]. On the positive side, SIDM also naturally predicts the very rapid formation of supermassive black holes [36, 37] via gravitational collapse of central (collisional) parts of DM halos [38, 39] — the process that is absent in the “vanilla CDM” paradigm. At last, the existence of the narrow plane of Andromeda dwarf satellites [40], which has no explanation within collisionless CDM, may potentially be addressed in SIDM, because collisionality induces viscous friction on subhalo motions in massive halos (whether its magnitude is enough remains to be seen).

However, an important possibility has been entirely missing from consideration so far, namely that a number of DM candidates are quantum flavor-mixed particles, e.g., a neutralino, an axion, a sterile neutrino, and others. In this Letter we demonstrate from the first principles via state-of-the-art N -body cosmological simulations that even the simplest model with two-component quantum-mixed DM with small mass-degeneracy agrees with observational data at both large and small scales, thus settling the above problems altogether. Moreover, it also agrees with observational constraints on the cross-section set by other collisional DM models [31–35]. At last, the model makes predictions for and is testable with direct and indirect detection DM experiments.

The physical idea is very simple. A mixed particle of a particular flavor α is a superposition of several mass-eigenstates $|f_\alpha\rangle = a_1|m_1\rangle + a_2|m_2\rangle + \dots$, where $|f\rangle$ and $|m\rangle$ denote wave-functions being flavor and mass eigenstates, and a_1, a_2, \dots are complex constants being elements of a unitary matrix. The dynamics of non-relativistic mixed particles has been shown to be rather unusual in that elastic scattering of mixed particles can lead to their irreversible escape from the gravitational potential well [41, 42] leaving nothing behind. This occurs because scatterings of particle mass eigenstates cause

their inter-conversions which change their kinetic (but not total) energy [41], thus giving a kick of the order of $v_k = c\sqrt{2\Delta m/m}$, where Δm is the mass difference of the mass eigenstates and c is the speed of light. This effect, referred to as the “quantum evaporation” (see Ref. [42] for a full quantum mechanical description) and suggested to occur in DM halos, can simultaneously soften the density cusps and reduce the number of subhalos. However, the structure on large scales where the escape velocities are much larger than v_k is unaffected.

Here we consider the simplest model of a flavor-mixed DM particle involving only two mass eigenstates and, correspondingly, two flavors [41, 42], i.e. the two-component dark matter (2cDM) model. The masses of the mass eigenstates are m_h and $m_l < m_h$, referred to as ‘heavy’ and ‘light’. Since mass eigenstates have different velocities, they propagate along different geodesics so they can be spatially separated by gravity during structure formation, when the characteristic (escape) velocities are of the order of v_k . Thereafter, DM halos are self-gravitating ensembles of non-overlapping heavy and light eigenstates.

A collisions of mass eigenstates can lead to either scattering or conversion, such as $|m_h\rangle \rightarrow |m_l\rangle$, or simply $h \rightarrow l$. Important conversions are $hh \rightarrow hl$, $hh \rightarrow ll$ and $hl \rightarrow ll$ (in which one or two heavy states are converted into the lighter states) because they increase particles’ velocities and lead to the quantum evaporation. Because of energy-momentum conservation, the kinetic energy of the eigenstates in heavy-to-light conversions increases by $\Delta mc^2 \equiv (m_h - m_l)c^2$ in processes like $hh \rightarrow hl$ and twice as much in $hh \rightarrow ll$. The reverse processes $hl \rightarrow hh$, $ll \rightarrow hl$ and $ll \rightarrow hh$ and can also occur if kinematically allowed, i.e., if kinetic energy is large enough to produce a heavy eigenstate. Finally, the scattering processes $ll \rightarrow ll$, $hl \rightarrow hl$ and $hh \rightarrow hh$ can occur as well, but there is always a set of parameters (the interaction strengths and the mixing angle) when they are vanishing [41, 42], hence they can be omitted in simulations when needed. Generally, any velocity-dependent cross-section, $\sigma(v)$, consistent with SIDM constraints, can equally well be utilized in the 2cDM model. Here we use the simplest one in which the conversion cross-section at low velocities is $\sigma(v) \propto 1/v^a$ with $a = 1$ (or greater) [42]. Such $1/v$ -dependence is not ruled out by observational data [29, 31, 39], so it is used in simulations reported here and $\sigma/m = 0.75 \text{ cm}^2/\text{g}$ at $v = v_k$ (for all conversion types) is also within the allowed range $0.1 \lesssim \sigma/m \lesssim \mathcal{O}(1) \text{ cm}^2/\text{g}$ at $v \sim 100 \text{ km/s}$ [29, 31, 39], where m is the characteristic mass of a DM particle, $m \simeq m_h$.

The physics of mixed-particle interactions was implemented in the cosmological TreePM/SPH publicly available code [43] Gadget-2. We simulate two types of DM particles representing h and l mass eigenstates; the total numbers of each type can change due to particle conversions. In order to implement interactions of DM particles, they are treated in the code as smooth-particle-

hydro (SPH) particles but without hydro-force acceleration. To model particles’ binary interactions, we use the Monte-Carlo technique together with the “binary collision approximation” [26, 28], which is reliable for weakly collisional systems. The Monte-Carlo particle interaction module works as follows. For each randomly chosen projectile particle, s_i , a nearest neighbor is found; this is the target particle, t_i (the subscript i stands for ‘initial’, i.e. before the interaction). This procedure identifies the type and velocity of each particle in the interacting pair, i.e., the input channel, $s_i t_i$ there always are four output channels, $s_f t_f$ (here f stands for ‘final’, i.e., after the interaction), namely: hh , hl , lh and ll . We compute the probabilities for each process $s_i t_i \rightarrow s_f t_f$ as follows:

$$P_{s_i t_i \rightarrow s_f t_f} = (\rho_{t_i}/m_{t_i}) \sigma_{s_i t_i \rightarrow s_f t_f} |\mathbf{v}_{t_i} - \mathbf{v}_{s_i}| \Delta t \Theta(E_{s_f t_f}) \quad (1)$$

where $\sigma_{s_i t_i \rightarrow s_f t_f} = \sigma$ is the cross-section which is assumed to be the same for all conversion channels and zero for scattering channels for 2cDM and vice versa for SIDM, $\mathbf{v}_{t_i} - \mathbf{v}_{s_i}$ is the relative velocity of particles in the pair, ρ_{t_i} is the density of target species, Δt is the iteration time-step and $\Theta(E_{s_f t_f})$ is the Heaviside function which ensures that the process is kinematically allowed (i.e., negative final kinetic energy, $E_{s_f t_f} < 0$, means the process cannot occur). Generally, $\sigma_{s_i t_i \rightarrow s_f t_f}$ depends on the mixing angle θ , so the above choice of σ ’s corresponds to maximal mixing $\theta = \pi/4$ for 2cDM and no mixing $\theta = 0$ for SIDM [42]. The densities ρ_{t_i} of each species at each particle’s position are computed using the appropriately modified density routine used in the SPH module of the original code. Whether an interaction occurs and through which channel it proceeds is determined by random drawing in accordance with the computed probabilities. If an interaction of any kind occurs, the pair kinematics is computed in the center of mass frame, where the momentum is conserved manifestly. If a scattering occurs, the particles are given random antiparallel velocities (in the center of mass frame) with magnitudes set by the energy and momentum conservation laws. If a conversion occurs, then (i) the type of one or both particles is changed accordingly, (ii) the magnitudes of the final velocities are computed accounting for the Δmc^2 given or taken, depending on the type of conversion and (iii) these velocities are assigned to particles in antiparallel directions in the center of mass frame. If no interaction occurs, the particle velocities and types remain intact. After this, the pair is marked inactive until the next time-step. This process is repeated for all active particles at each time step.

Simulations reported here were performed using XSEDE high performance computing systems *Trestles* and *Ranger*. The 2cDM runs have $2 \times 400^3 = 128$ million SPH-DM particles (in 2cDM, the initial numbers of h and l particles are equal) in the box of $50h^{-1} \text{ Mpc}$

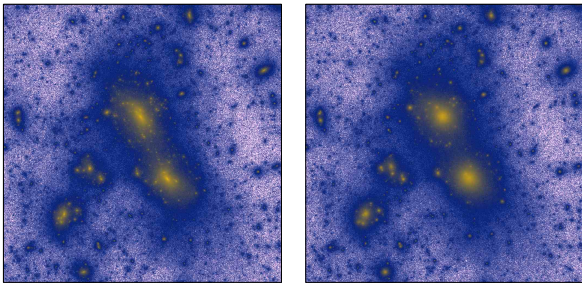


FIG. 1. Dark matter distribution in a region of size $5h^{-1}$ Mpc with the standard Λ CDM (left panel) and the 2cDM (right panel) model with $\sigma/m = 0.75 \text{ cm}^2/\text{g}$, $v_k = 50 \text{ km/s}$. Both these simulations have the same number of particles. Note the deficit of substructure (small yellow clumps) in the 2cDM vs Λ CDM model.

(comoving) with the force resolution scale of $3.5h^{-1} \text{ kpc}$, and the reference Λ CDM run has $2 \times 640^3 \approx 524$ million particles and the force resolution of $2.2h^{-1} \text{ kpc}$. Our box size was optimized to be large enough to be a representative sample the universe volume, yet it provides reasonable resolution at small scales. All the runs are DM-only simulations using the standard cosmological parameters $\Omega_m = 0.3, \Omega_\Lambda = 0.7, \Omega_b = 0$ and $h = 0.7$. Initial conditions are generated using N-GenIC code with the Eisenstein-Hu spectrum model, with $\sigma_8 = 0.9$ and the initial redshift $z = 50$. Post-processing was done with AHF code [44], which was used to construct the halo mass and velocity functions, analyze halo density profiles, etc. Simulations of SIDM have also been done for the same cosmological parameters. They fully confirm earlier studies, e.g., the inability to resolve the substructure problem, hence these results are not reported here. A number of simulations were performed to explore a range of the 2cDM model parameters $\Delta m/m$ and σ/m , to compare with the reference CDM and SIDM models and to check for numerical convergence. All the results will be reported in detail elsewhere; here we show the most important ones.

Simulations with large mass difference $m_h \geq m_l$ (not presented here) show the enhancement of substructure relative to the large-scale halos (masses large halos are diminished to produce more smaller ones). This makes the substructure problem worse and, hence rules out the non-degenerate case. We focus on the degenerate case $m_l \simeq m_h = m$ hereafter.

The representative case of the DM distribution at $z = 0$ for the 2cDM and Λ CDM models are presented in Fig. 1, which show the zoomed-in region of 5 Mpc across. One can see the reduced number of subhalos and the less concentrated central parts in the 2cDM case. The 2cDM parameters used are $\Delta m/m \simeq 10^{-8}$, which corresponds to $v_k = 50 \text{ km/s}$, and $\sigma/m = 0.75 \text{ cm}^2/\text{g}$ at $v = v_k$, which is fully consistent with observational constraints

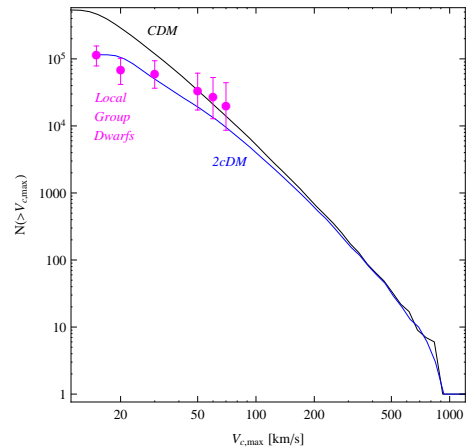


FIG. 2. The maximum circular velocity function for the standard Λ CDM model (black curve) and the 2cDM model with $v_k = 50 \text{ km/s}$ and $\sigma/m = 0.75 \text{ cm}^2/\text{g}$ (blue curve). The 2cDM provides an excellent fit to the appropriately scaled Local Group data [2, 4] (magenta points).

on the SIDM cross-section [29–34, 39]. For these values, the 2cDM circular velocity function matches the Local Group data the best, as is illustrated in Fig. 2. This figure shows the number of halos with the maximum circular velocity above a certain value, $N(> V_{c,\text{max}})$ versus $V_{c,\text{max}}$, for 2cDM and Λ CDM; the data points are from [2, 4]. The amount of substructure is volume-dependent, so we appropriately renormalized the data points to reproduce the results of Refs. [2, 4] using the velocity function from our Λ CDM simulation; the procedure is legitimate for a scale-free ergodic distribution of DM substructure. Scanning through the 2cDM model parameters, we have found that v_k uniquely determines the position of the break in the velocity function, $V_{c,\text{max}}^{\text{break}} \simeq v_k$, whereas σ/m determines the slope below the break. Comparison with observations determines v_k rather accurately to be around $\sim 50 - 70 \text{ km/s}$. Interestingly, a similar value of a characteristic velocity $\lesssim 100 \text{ km/s}$ was found in another independent analysis of survey data [5]. The ‘best fit’ cross-section is $\sigma/m \sim 0.75 \text{ cm}^2/\text{g}$ at v_k but values a factor of two smaller or larger are marginally acceptable too. The halo mass function exhibits even sharper break at halo masses $M \simeq 10^{10} M_\odot$. Thus, the overall suppression of the subhalo abundance at small velocities and masses resolves the “missing satellite problem”.

Fig. 3 shows the Λ CDM and 2cDM halo density profiles. Plotted are over one hundred of well-resolved profiles, the inner parts of them were truncated according to the numerical binary collision criterion [45], hence they are trustworthy everywhere. The Λ CDM profiles agree with the NFW profile. In contrast, the 2cDM inner profiles are less centrally concentrated and shallower (and some are core-like), as is also seen from Fig. 4. Here, the effective power-law index is obtained by fitting the

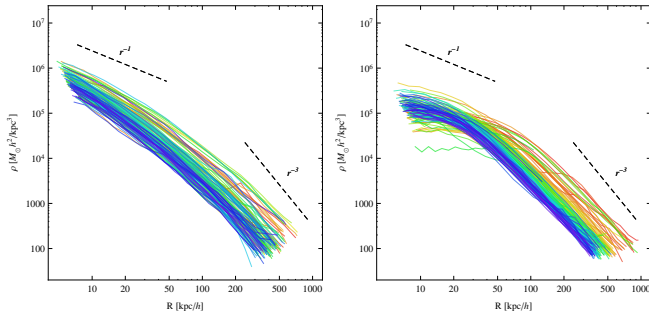


FIG. 3. Density profiles of 120 well-resolved dark halos are plotted for the classical Λ CDM (left panel) and two 2cDM models. The profiles are color-coded by the halo mass: red – most massive, blue – less massive.

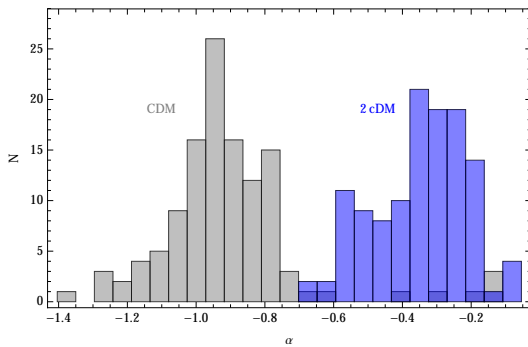


FIG. 4. Histograms of the slopes of the inner density profiles of the halos shown in Fig. 3. Whereas the CDM profiles show a cusp r^α with $\alpha \sim -0.8 \dots -1$ consistent with earlier studies, the 2cDM profiles are much shallower: $\alpha \sim -0.2 \dots -0.6$.

profiles with the function $\rho = \rho_0 r^\alpha (1 + r/r_c)^\beta$ and then evaluating α at $r = 7 \text{ kpc}/h$. The distribution of the slopes ranges within $\alpha \simeq -0.8 \dots -1$ for CDM indicating a cusp and within $\alpha \simeq -0.2 \dots -0.6$ for 2cDM, which thus explains the “core-cusp problem” and, likely, the “too big to fail problem”. However, there is large diversity in the values of the central density and the inner slopes due to different formation histories in agreement with a ‘counter-example’ study [21]. Importantly, density profiles and the core sizes of massive halos are mostly sensitive to the value of σ/m , the value of v_k plays little role, if any. The profiles of smaller halos with masses around or below $10^{10} M_\odot$ can be sensitive to v_k . Dedicated high-resolution simulations are needed to study this in detail.

The 2cDM theory is testable with direct detection experiments. Indeed, DM is a collection of h and l species and they can convert into one another when they interact with normal matter in a detector. These conversions will result in energy ‘mismatch’ of $\sim \Delta m c^2$, i.e., the events will look like inelastic collisions. Down-conversions $h \rightarrow l$ should always occur, along with elastic scatterings, and will result in additional recoil energy. In contrast, up-conversions $l \rightarrow h$ will result in the deficit of energy and

can occur only if kinetic energy is enough. Since v_k is comparable to the velocity of Earth around the Sun and of the Sun in the Galaxy, annular modulation of conversion rates is expected. The absolute value of Δm is not constrained by our analysis, but only the relation $\Delta m \simeq 10^{-8} m$. If inelastic effects are responsible for DAMA and CoGeNT anomalies, then $\Delta m \sim \text{few keV}$. Then the DM mass should be $m_X \sim \text{few} \times 10^2 \text{ GeV}$, which consistent with $m_X \sim 130 \text{ GeV}$ from possible annihilation gamma-ray line found in *Fermi* LAT data [46].

To summarize, cosmological N -body simulations with two-component DM have been performed for the first time and show different structure formation on small scales. The 2cDM model does not change the linear power spectrum (unlike warm DM); all the changes occur in the nonlinear stage. The results are as follows. First, cosmology with at least two mixed DM species with high mass degeneracy, $\Delta m/m \sim 10^{-8}$, is preferred. In turn, self-interacting DM models with single species (e.g., non-flavor-mixed) candidates such as gravitino and others and non-degenerate multi-component DM models are disfavored. Second, 2cDM has a reduced amount of dwarf halos with masses below $10^{10} M_\odot$ and typical velocities smaller than 50–70 km/s, hence it resolves the “substructure” problem. Third, 2cDM softens central cusps and makes halos less centrally concentrated, thus solving the “core-cusp” and “too big to fail” problems in the same way SIDM does. 2cDM agrees with observations within a range of velocity-dependent cross-section allowed for SIDM [29–34, 39]. The constraints are tight: if σ is too small, then it is cosmologically uninteresting, if it is too large, then the cusps will be enhanced due to gravothermal collapse of halos. This fine tuning, rephrased as “Why now?” question is a caveat of 2cDM model. However, SIDM and dark energy/cosmological constant face the same problem. Whether they are related remains to be seen. Fourth, being a collisional model, akin to SIDM, 2cDM can also explain the existence of supermassive black holes at high- z via semi-collisional DM accretion [38]. Fifth, 2cDM passes the early universe constraint – that at high densities higher mass particles must convert into the lightest one – because the conversion cross-section in flat space-time is suppressed by $(\Delta m/m)^4 \sim 10^{-32}$ over its current value [42]. Sixth, conversions can be seen in direct detection DM experiments as inelastic (endothermic or exothermic) processes with $\Delta E \simeq \pm \Delta m c^2$ or twice as much. Seventh, we predict that evaporation of dwarf halos should enrich the environment with metals from stars formed earlier in these halos, which would mimic the effect of supernova feedback. Since not all the small halos are evaporated, the residual substructure can be responsible for flux anomalies in gravitational lensing observations.

This work was supported in part by grants DE-FG02-07ER54940 (DOE), AST-1209665 (NSF) and XSEDE AST110024 and AST110056 at TACC and SDSC.

* mmedvedev@cfa.harvard.edu

† Also at the Department of Physics and Astronomy, University of Kansas, Lawrence, KS 66045; Also at the ITP, NRC “Kurchatov Institute”, Moscow 123182, Russia

- [1] Bertone, G., Hooper, D., & Silk, J., *Phys. Rep.*, **405**, 279 (2005).
- [2] Klypin, A., Kravtsov, A.V., Valenzuela, O., & Prada, F., *Astrophys. J.*, **522**, 82 (1999).
- [3] Moore, B., Ghigna, S., Governato, F., Lake, ., Quinn, T., Stadel, J., & Tozzi, P., *Astrophys. J. Lett.*, **524**, L19 (1999).
- [4] Kravtsov, A., *Advances in Astronomy*, 2010, doi:10.1155/2010/281913 (2010).
- [5] Zwaan, M.A., Meyer, M.J., & Staveley-Smith, L., *Montly Not. R. Astron. Soc.*, **403**, 1969 (2010).
- [6] Papastergis, E., Martin, A. M., Giovanelli, R., & Haynes, M. P., *Astrophys. J.*, **739**, 38 (2011).
- [7] Navarro, J.F., Frenk, C.S., & White, S.D.M., *Astrophys. J.*, **490**, 493 (1997).
- [8] de Blok, W. J. G., Walter, F., Brinks, E., Trachternach, C., Oh, S-H., & Kennicutt, Jr., R. C., *Astrophys. J.*, **136**, 2648 (2008).
- [9] de Blok, W.J.G., *Advances in Astronomy*, 2010, doi:10.1155/2010/789293 (2010).
- [10] Kuzio de Naray, R., & Kaufmann, T., *Montly Not. R. Astron. Soc.*, **414**, 3617 (2011).
- [11] Newman, A.B., Treu, T., Ellis, R.S., Sand, D.J., Richard, J., Marshall, P.J., Capak, P., & Miyazaki, S., *Astrophys. J.*, **706**, 1078 (2009).
- [12] Boylan-Kolchin, M., Bullock, J. S., & Kaplinghat, M., *Montly Not. R. Astron. Soc.*, 415, L40 (2011).
- [13] Boylan-Kolchin, M., Bullock, J. S., & Kaplinghat, M., *Montly Not. R. Astron. Soc.*, **422**, 1203 (2012).
- [14] Governato, F., Brook, C., Mayer, L., et al., *Nature*, **463**, 203 (2010).
- [15] Walker, M.G., & Peñarrubia, J., *Astrophys. J.*, **742**, 20 (2011).
- [16] Ferrero, I., Abadi, M.G., Navarro, J.F., Sales, L.V., & Gurovich, S., *Montly Not. R. Astron. Soc.*, **425**, 2817 (2012).
- [17] Peñarrubia, J., Pontzen, A., Walker, M. G., & Kaposov, S. E., *Astrophys. J. Lett.*, 759, L42 (2012).
- [18] Garrison-Kimmel, S., Rocha, M., Boylan-Kolchin, M., Bullock, J., & Lally, J., arXiv:1301.3137 (2013).
- [19] Avila-Reese, V., Colín, P., Valenzuela, O., D’Onghia, E., & Firmani, C., *Astrophys. J.*, **559**, 516 (2001).
- [20] Bode, P., Ostriker, J. P., & Turok, N., *Astrophys. J.*, **556**, 93(2001).
- [21] Kuzio de Naray, R., Martinez, G.D., Bullock, J.S. & Kaplinghat, M., *Astrophys. J. Lett.*, **710**, L161 (2010).
- [22] Villaescusa-Navarro, F., & Dalal, N., *J. Cosmol. Astropart. Phys.*, **3**, 24 (2011).
- [23] Macciò, A. V., Paduroiu, S., Anderhalden, D., Schneider, A., & Moore, B., *Montly Not. R. Astron. Soc.*, **424**, 1105 (2012).
- [24] Carlson, E. D., Machacek, M. E., & Hall, L. J., *Astrophys. J.*, **398**, 43 (1992).
- [25] Spergel, D.N., & Steinhardt, P.J., *Phys. Rev. Lett.*, **84**, 3760 (2000).
- [26] Burkert, A., *Astrophys. J. Lett.*, **534**, L143 (2000).
- [27] Yoshida, N., Springel, V., White, S.D.M., & Tormen, G., *Astrophys. J. Lett.*, **544**, L87 (2000).
- [28] Davé, R., Spergel, D.N., Steinhardt, P.J., & Wandelt, B.D., *Astrophys. J.*, **547**, 574 (2001).
- [29] Colín, P., Avila-Reese, V., Valenzuela, O., & Firmani, C., *Astrophys. J.*, **581**, 777 (2002).
- [30] Ahn, K., & Shapiro, P.R., *Montly Not. R. Astron. Soc.*, **363**, 1092 (2005).
- [31] Randall, S.W., Markevitch, M., Clowe, D., Gonzalez, A.H., & Bradač, M., *Astrophys. J.*, **679**, 1173 (2008).
- [32] Arkani-Hamed, N., Finkbeiner, D.P., Slatyer, T.R. & Weiner, N., *Phys. Rev. D*, **79**, 015014 (2009).
- [33] Loeb, A. & Weiner, N., *Phys. Rev. Lett.*, **106**, 171302 (2011).
- [34] Vogelsberger, M., Zavala, J., & Loeb, A., *Montly Not. R. Astron. Soc.*, **423**, 3740 (2012).
- [35] Zavala, J., Vogelsberger, M., & Walker, M. G., *Montly Not. R. Astron. Soc.*, **431**, L20 (2013).
- [36] Willott, C. J., Delorme, P., Omont, A., et al., *Astron. J.*, **134**, 2435 (2007).
- [37] Treister, E., Schawinski, K., Volonteri, M., Natarajan, P., & Gawiser, E., *Nature*, **474**, 356 (2013).
- [38] Ostriker, J. P., *Phys. Rev. Lett.*, **84**, 5258 (2000).
- [39] Hennawi, J. F., & Ostriker, J. P., *Astrophys. J.*, **572**, 41 (2002).
- [40] Ibata, R.A., et al., *Nature*, **473**, 62 (2013).
- [41] Medvedev, M.V. *J. Phys. A: Math. General*, **43**, 2002 (2010).
- [42] Medvedev, M.V., *Phys. Rev. D*, submitted; arXiv:1305.???? (2013).
- [43] Springel, V., *Montly Not. R. Astron. Soc.*, **364**, 1105 (2005).
- [44] Knollmann, S.R., & Knebe, A., *Astrophys. J. Suppl.*, **182**, 608 (2009).
- [45] Power, C., Navarro, J.F., Jenkins, A., Frenk, C.S., White, S.D.M., Springel, V., Stadel, J., & Quinn, T., *Montly Not. R. Astron. Soc.*, **338**, 14 (2003).
- [46] Weniger, C., *J. Cosmol. Astropart. Phys.*, 8, 7 (2012)